Water Research 219 (2022) 118555

Contents lists available at ScienceDirect

Water Research

journal homepage: www.elsevier.com/locate/watres

# Characterising sedimentation velocity of primary waste water solids and effluents

Kareem Abood [*,a], Tanmoy Das [c,d], Daniel R. Lester [c], Shane P. Usher [b], Anthony D. Stickland [b], Catherine Rees [e], Nicky Eshtiaghi [c], Damien J. Batstone [a]

[a] Australian Centre for Water and Environmental Biotechnology, The University of Queensland, St. Lucia, Brisbane, 4072, Queensland, Australia
[b] ARC Centre of Excellence for Enabling Eco-Efficient Beneficiation of Minerals, Department of Chemical Engineering, The University of Melbourne, Grattan St, Parkville, Melbourne, 3010, Victoria, Australia
[c] School of Engineering, RMIT University, 124 La Trobe St., Carlton, Melbourne, 3000, Victoria, Australia
[d] Department of Chemical Engineering, The University of Melbourne, Victoria 3010, Australia
[e] Melbourne Water Corporation, 990 La Trobe St., Docklands, Melbourne, 3008, Victoria, Australia

ARTICLE INFO

*Keywords:*
Polydisperse sludge
Sedimentation
Computational fluid dynamics
Monte Carlo
OpenFOAM®
Dakota®
Python®

ABSTRACT

Sedimentation in waste water is a heavily studied topic, but mainly focused on hindered and compression settling in secondary sludge, a largely monodispersed solids, where bulk sedimentation velocity is effectively described by functions such as double Vesilind (Takacs). However, many waste water solids, including primary sludge and anaerobic digester effluent are polydispersed, for which application of velocity functions is not well understood. These systems are also subject to large concentration gradients, and poor availability of settling velocity functions has limited design and computational fluid dynamic (CFD) analysis of these units. In this work, we assess the use of various sedimentation functions in single and multi-dimensional domains, comparing model results against multiple batch settling tests at a range of high and low concentrations. Both solids concentration and sludge bed height (interface) over time are measured and compared. The method incorporates uncertainty analysis using Monte Carlo regression, DIRECT (dividing rectangles), and Newton optimisation. It was identified that a double Vesilind (Takacs) model was most effective in the dilute regime ($< 1\% v/v$), but could not effectively fit high solids concentrations ($> 1\% v/v$) without a substantial (50%) decrease in effective maximum sedimentation velocity ($V_0$). Other parameters ($R_h$, $R_p$) did not change. A power law velocity model (Diehl) was significantly less predictive at low concentrations, and not significantly better at higher concentrations. The optimised model (with reduction in $V_0$) was tested vs a standard (optimised) double Vesilind velocity model in a simple primary sedimentation unit, and resulted in deviation from -12% to +18% in solids capture prediction from underload to overload (washout) conditions, indicating that the effect is important in CFD based analysis of these systems.

## 1. Introduction

Sedimentation of particulate species is a critical process in the waste water treatment industries, especially in the context of secondary settling. In these processes, hindered settling occurs where the suspension sedimentation velocity is less than the free settling velocity of an isolated particle due to particle-particle hydrodynamic interactions and upflow of the suspending fluid. When the suspension particles are relatively uniform in size (e.g., activated sludge, secondary sludges), this results in a clear zone (supernatant), a hindered settling zone (type 3), and a compression zone (type 4) (Tchobanoglous et al., 2014). A sharp interface can often be observed between the hindered settling zone and the supernatant. Although particle velocity fluctuations can potentially generate dispersion around this interface, in practice these fluctuations are mitigated by local hindered settling that maintains a well-defined interface (Guazzelli and Hinch, 2011; Tee et al., 2002) generating a

* Corresponding author. Postal address: Australian Centre for Water and Environmental Biotechnology, Level 4 Gehrmann Building, The University of Queensland, Brisbane Qld 4072, Australia.
*E-mail addresses:* K.Abood@uq.net.au (K. Abood), s3696708@student.rmit.edu.au (T. Das), daniel.lester@rmit.edu.au (D.R. Lester), spusher@unimelb.edu.au (S.P. Usher), stad@unimelb.edu.au (A.D. Stickland), catherine.rees@melbournewater.com.au (C. Rees), nicky.eshtiaghi@rmit.edu.au (N. Eshtiaghi), d.batstone@uq.edu.au (D.J. Batstone).

https://doi.org/10.1016/j.watres.2022.118555
Received 4 February 2022; Received in revised form 25 April 2022; Accepted 3 May 2022
Available online 5 May 2022

characteristic mean sedimentation velocity. This sedimentation velocity depends on the local solids concentration and is independent of container shape or size (Batchelor, 1972; Hinch, 1977). In batch settling tests, the suspension/supernatant interface height can be tracked over time to generate flux-concentration curves (Diehl, 2007; Lester et al., 2005) or extract parameters for velocity-concentration models (Cole, 1968; Kynch, 1952; Richardson, 1954; Takacs et al., 1991; Vesilind, 1968), either of which can be subsequently be used for prediction and design of sedimentation processes. Therefore, determining the sedimentation characteristics of activated and secondary sludges from batch settling tests is a robust and straightforward process.

Conversely, suspensions with significantly non-uniform particle size, shape and density distributions, such as anaerobic sewage treatment effluent and primary settling tanks sludges are much more challenging to characterise. First, the sedimentation velocity of each species is a function of the local solids concentration of all other species. Instead of a sharp visible interface between the clear and hindered zone, there is usually a solids concentration gradient due to the continuous range of settling velocities of the isolated particles that comprise these polydisperse systems. The sedimentation dynamics of such strongly polydisperse suspensions can be very complex as they can exhibit strong particle segregation and stratification (Bürger et al., 2002), complex flow structures during sedimentation (Nguyen and Ladd, 2005), and increased velocity fluctuations and dispersion near interfaces (Guazzelli and Hinch, 2011; Nguyen and Ladd, 2005). Polydisperse suspensions can also exhibit fundamentally different sedimentation dynamics (Batchelor, 1982; Batchelor and Van Rensburg, 1986; Bürger et al., 2002) that range from ”stable” (where particles in each class are homogeneously distributed horizontally) to ”unstable” (where different particles classes form vertical columnar structures that give rise to a localised Boycott effect).

Regardless of sedimentation stability, macroscopic models of polydisperse sedimentation are typically couched in terms of a characteristic mean sedimentation velocity for each particle class (i.e. size, shape, density) which may be represented as discrete classes (Bürger et al., 2002) or a continuous spectrum (Bürger et al., 2008). These sedimentation velocities depend upon the solids concentration of the relevant particle class and the total local solids concentration (Batchelor, 1982; Lockett and Bassoon, 1979; Masliyah, 1979). In either case, the determination of the sedimentation velocity of each particle class from experimental observations (even for simple model systems such as bidisperse suspensions) is currently an open problem. Conversely, waste water treatment applications require accurate and straightforward methods to characterise the sedimentation velocity of primary sludges and effluents to facilitate quantification, design and optimisation of industrial sedimentation processes.

Thus, the challenge is to develop practical, robust and accurate tools and techniques to characterise the sedimentation velocity of these complex suspensions from dilute to highly concentrated solids concentrations. For these reasons, empirical relationships are typically used for design (Tchobanoglous et al., 2014) which do not require concentration-velocity functions (and do not rely on the dimensional analysis), or application of a mono-disperse assumption, with limited ability to measure parameters. This results in a more limited design approach, and means that computational fluid dynamics cannot be adequately used for design and analysis, even post-hoc, since velocity-concentration models are fundamental to this analysis (Samstag et al., 2016). Furthermore, there is limited understanding of whether a monodispersed assumption is appropriate for these types of suspensions. As the rheology and mechanical properties of waste water sludges vary enormously (non-linearly) with solids concentration (Eshtiaghi et al., 2013; Stickland, 2015), then minor errors in the characterisation of sedimentation velocity (and thus predicted solids concentration distribution) can lead to significant errors in modelling and prediction of waste water treatment processes. These issues currently hinder model-based design and analysis of industrial processes, including primary settlers, anaerobic lagoons and sewage systems.

Hindered settling models commonly used for secondary sludges are characterised in terms of the empirical functional forms used to describe solids settling velocity as a function of concentration. The first model type uses an exponential function of solids concentration (Vesilind, 1968) which was subsequently extended by Takacs et al. (1991) to incorporate a second exponential term to improve prediction at low concentrations (double Vesilind). This is the most widely used model for the simulation of sedimentation in secondary and primary sludge applications (Brennan, 2001; Gernaey et al., 2001; Lakehal et al., 1999; Ramin et al., 2014). Although the Takacs model is designed for polydisperse suspensions, it does not resolve the higher solids concentration behaviour, as it focuses on dilute and hindered zones. The combined HTC model (Hindered, Transient and Compression) proposed by Ramin et al. (2014) utilises Vesilind exponential settling functions coupled with a simple model for compression once the sludge forms a continuous solids matrix (gel point). This model was used to simulate sedimentation and consolidation of a secondary sludge material to an acceptable degree of accuracy over the entire expressed solids concentration range. Model parameters are estimated by tracking the evolution of the suspension/supernatant interface over time and so is limited to secondary and activated sludge.

The second model type utilises a power law for the velocity-concentration relationship (Cole, 1968), such as the Richardson-Zaki law (Richardson, 1954) which corresponds to analytic expressions for sedimentation of colloidal spheres in the dilute limit (Batchelor, 1977; Hinch, 1977). As such, power-law functions have been used extensively in applications of the theory of sedimentation and consolidation of colloidal suspensions (Bürger, 2000; Buscall and White, 1987), and more recently these functional forms have been used to characterise the sedimentation of activated sludge (De Clercq et al., 2008; Plósz et al., 2007; Torfs et al., 2017). When combined with an appropriately-characterised model for sludge compression, the power-law sedimentation velocity function is particularly effective in describing compression zone settling in secondary settling tanks (Bürger et al., 2011; Stickland, 2015).

The vast majority of waste water sedimentation characterisation methods have focused on secondary waste water sludges, which have been used to model the total solids concentrations in secondary settlers and clarifiers. Conversely, accurate sedimentation characterisation methods for primary waste water sludges are an outstanding challenge (Brennan, 2001; Dahl, 1995; Griborio et al., 2014; Liu and García, 2011). In many cases, models developed for secondary sludges are applied to primary sludges without any testing or further modification, most commonly using (Takacs et al., 1991) without adding a compression component (Brennan, 2001; Liu and García, 2011). Only limited studies to date (Ramin et al., 2014) have focused on characterising sedimentation that could be used in the dilute and concentrated regimes, but these have not been validated in the full range of solids concentration, particularly in dilute regions. Hence robust and accurate characterisation methods are required to facilitate accurate prediction, design and optimisation of high solids gradient sludge process units. The challenge associated with such types of sludges is that they are highly polydisperse, leading to complex sedimentation behaviours and an absence of a well-defined sediment/supernatant interface that is often used as a key data source for characterisation (Diehl, 2007; Kynch, 1952; Lester et al., 2005). Furthermore, it is also clear that conventional polydisperse sedimentation models are too complex to facilitate robust characterisation. Hence an important research question is whether simplified characterisation methods (based upon e.g. a monodisperse paradigm or variations thereof) are appropriate for high solids concentration range sludges. Sedimentation velocity is generally characterised in batch sedimentation tests (Tchobanoglous et al., 2014), and parameters are generally identified using a 1D model (Takacs et al., 1991; Tchobanoglous et al., 2014). Clarifier process models are almost always

1D (normally using a Takacs model), while CFD is most commonly done in 2D (with 3D being increasingly used) (Griborio et al., 2022). As sedimentation is an inherently unstable process due to strong gravity currents (even in the monodisperse case), it remains unclear whether a 3D sedimentation model that resolves these currents can result in a different characteristic settling velocity than the 1D/2D case. The majority of sedimentation studies do not assess simplification to 1D or 2D in either batch sedimentation, or lab, or full-scale process applications. Finally, only a small number of conventional sedimentation characterisation methods have been validated or have incorporated uncertainty analysis, limiting the development of model-based design tools.

In this study, we attempt to address the above challenges by developing and testing a robust and accurate method for characterisation of the sedimentation velocity of primary sludges and effluents. Method development is based upon CFD modelling and batch sedimentation tests performed upon a polydisperse sludge sampled from an anaerobic lagoon of a major waste water treatment facility. This sludge is representative of polydispersed solids (including primary sludge) in that it does not exhibit a clear interface during batch sedimentation, and the solids concentration range expressed in these tests is broader than that of primary settlers. Starting with conventional sedimentation and compression models for monodisperse suspensions, exponential and power law models, with and without compression are optimised and parameter uncertainty estimated in both high and low solids using an algebraic slip (i.e., drift-flux) CFD approach. The models are then tested in a continuous flow pilot clarifier system at under-load, normal, and overload (washout conditions) to identify the sensitivity of actual systems to the models identified.

## 2. Materials and methods

### 2.1. Materials

Sludge samples were collected from an anaerobic lagoon treating municipal sewage located in Melbourne, Victoria, Australia. The sludge had total solids content of 6.7 wt% with a volatile solids fraction (or total solids) of 61%. The total solids content of the sample was determined according to APHA 2540B (105 °C for 24 h) (APHA, 2005). Volatile solids content of the sample was measured according to APHA 2540E (550 °C for 2 h) (APHA, 2005). The total dissolved solids content was 0.108 wt% and the solids density was 1829 $kg/m^3$. Dissolved solids was measured by filtration through a 0.22μm cellulose acetate membrane followed by oven drying at 105 °C for 24 h. The solids density of the sample was calculated from the measured values of density and solids concentration of the suspension, and density and total dissolved solids content. High concentration sludge was obtained from the centrifugation of sample at 3500 rpm for 2 h in a Beckman Coulter Allegra X-12 centrifuge. Suspension density was measured using a calibrated density cup, whereas the liquor density was measured using a calibrated pycnometer.

### 2.2. Methods

#### 2.2.1. Novel characterization approach

To identify the capability of models to effectively describe polydisperse sedimentation behaviour across a broad solids range, we developed tests at both low and high solids concentrations. The tests conducted measured change in 1-D solids concentrations at different heights over time in the low concentration range, and sludge bed height over time in the high concentration range. These were then simulated using open source CFD software (OpenFOAM).

The dilute tests are assessed initially, with all three candidate models (Diehl, 2015; Takacs et al., 1991; Vesilind, 1968) optimised and assessed on this system (3 tests with 3 different initial conditions), which includes parameter uncertainty quantification. These models are then tested on the high concentration tests (incorporating compression) and the optimal model parameters and confidence regions assessed. Ideally, confidence regions for dilute and concentrated ranges should overlap, which would indicate the model is valid across the whole range. As noted in the results, this was not the case, but effectively only one parameter was impacted by the change in concentration.

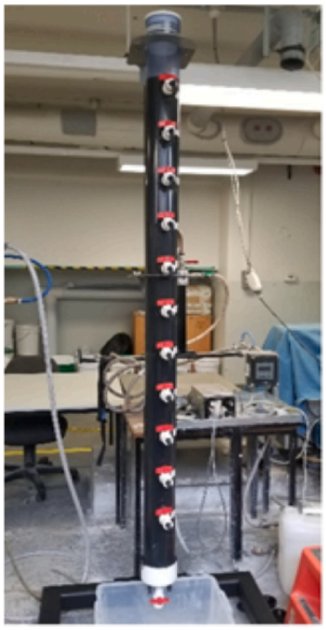

**Fig. 1.** Experimental dilute batch settling column.

#### 2.2.2. Dilute settling test

Dilute settling experiments were conducted in a 2 m high cylindrical column with an outer diameter of 100 mm shown in (Fig. 1). The cylindrical column had sampling ports on one side (15 mm diameter valves). The first sampling port was 250 mm from the base, and there were 10 more sampling ports spaced evenly (150 mm apart). The top sampling port was 250 mm from the top of the column. There was a valve at the base of the column to facilitate drainage and cleaning. Feed samples for the experiment were prepared by diluting the concentrated sludge samples using liquor free of any suspended solids to the three initial conditions of 3.86 g/L, 4.75 g/L, and 5.76 g/L.

At the beginning of the dilute settling experiment 15 *kg* of diluted sludge sample was poured into the cylindrical pipe from the top. A timer was started as soon as the sample loading was completed and samples were drawn from each port (except the top two ports) at five minutes intervals for the first thirty minutes and at ten minutes intervals for the next thirty minutes. After ten minutes, no samples were drawn from the top two ports. The total suspended solids and weight of each sample were measured. The volume loss from drawing samples were recorded for each sample, with time stamp, to include in the 3D model and evaluate the impact of sampling on sedimentation behaviour.

#### 2.2.3. Concentrated batch settling test

Concentrated settling tests were conducted at lower concentrations than as-received sludge by diluting the samples with their own liquor down to (0.7-0.85 vol%) (1.258-1.543 wt%). The lower limit of 1.258 wt % was the minimum high solids concentration for that material to have an optically observable defined solids-liquid interface. At concentrations higher than 1.543 wt%, sedimentation was excessively slow, which resulted in autogenic gas production, which disrupted the test. The liquor was obtained from the centrifugation of sample at 3500 rpm for 2 h in a Beckman Coulter Allegra X-12 centrifuge. The solids volume fraction was calculated from the suspended solids content, and the solids

and liquor densities. The samples were poured into a 500 mL measuring cylinder and the solid-liquid interfacial height was recorded over time using a video camera. Visual observations of interface height during the test and video recordings were used to develop a solid-liquid interface height profile over time.

### 2.3. Modelling approach

#### 2.3.1. Fluid dynamics and physics

OpenFOAM was used as a CFD simulation platform; specifically, a multi-phase based numerical solver utilising algebraic slip (drift flux) between the phases. The drift flux approach models different phases as a variable density heterogeneous mixture and solves for both the mixture velocity and solids concentration, where the drift flux of the solids phase relative to the mixture velocity is given by the concentration-dependent sedimentation velocity functions as provided below. The mixture has a continuous phase, water in this case, and one or more dispersed phases which are subject to sedimentation velocity in addition to continuous phase convection. The sedimentation velocity function combined with the mixture approach incorporates momentum transfer between the phases implicitly. The alternative approach (Euler-Euler) would require simulation of multiple separate phases and an explicit sedimentation function with momentum transfer considered separately, which increases the complexity of the solver and required computational cost, and makes the use of empirical sedimentation functions more difficult.

The default turbulence model used is a modified k-$\epsilon$, with buoyancy term described in Brennan (2001) and Lakehal et al. (1999). The model takes mixture viscosity as input then adds the turbulence contribution. The buoyancy term is based on the density gradient generated from the mixture composition. Based on test cases in (Fig. 3), it was determined that the effect of turbulence is negligible due to the extremely slow velocity in the experimental cases. However a similar modification as in Brennan (2001) was done to a standard k-$\omega$ SST and LES (Large Eddy simulation) (Smagorinsky, 1963) models which proved to be more numerically stable than the original modified k-$\epsilon$ model. Those models were utilized in some of the 3D simulations.

The default rheology model in the Open FOAM drift Flux model is a Bingham plastic mixture viscosity model from Brennan (2001) and Dahl (1995). Model parameters are a function of solids concentration. Dahl (1995) identifies that this should be improved for large scale predictions. However, several test cases were optimised and fitted using the default model and a specifically fitted model for the material using a Herschel Bulkley model. Differences were marginal due to the low velocity profiles overall.

#### 2.3.2. Sludge sedimentation models

In this section we consider conventional models for sludge sedimentation, some of which are extended to account for non-settling fractions. The first model under consideration is the classical Vesilind model (Vesilind, 1968) which uses a single exponential function for the sedimentation velocity $V_s$:

$$V_s(C) = V_0 e^{-R_h C}. \tag{1}$$

Here $C$ [g/L] represents the suspended solids concentration, $V_0$ [m/s] is the maximum sedimentation velocity ($C \to 0$), and $R_h$ [l/g] is a parameter that characterises hindering of sedimentation velocity with increasing solids concentration. This model was implicitly developed for monodisperse suspensions, as the functional form Eq. (1) quantifies hindered settling in terms of a single unique sedimentation velocity that only depends upon the total solids concentration. The Vesilind model was extended by Takacs et al. (1991) to account for the presence of different particle fractions in polydisperse suspensions. It was considered that the suspension consists of three broad classes of particles: a non-setting fraction $C_{\min}$ of small particles, a range of poor settling particles, and a range of rapidly settling particles. This leads to a sedimentation velocity model of the form

$$V_s(C) = \begin{cases} 0 & C < C_{\min}, \\ V_0\left(e^{-R_h(C-C_{\min})} - e^{-R_p(C-C_{\min})}\right) & C \geqslant C_{\min}. \end{cases} \tag{2}$$

Where $C_{\min}$ represents the concentration of non-settling particles, and the additional parameter $R_p$ [l/g] (with $R_p > R_h$) characterises sedimentation in the low solids concentration range. This implicitly polydisperse sedimentation model is markedly different to the Vesilind model in Eq. (1) in that a non-settling fraction $C_{\min}$ is accounted for, and the sedimentation velocity is non-monotonic, increasing from zero at $C = C_{\min}$ to a maximum value at intermediate solids concentrations, before decaying exponentially at large $C$. We also consider the power law sedimentation model proposed by Diehl (2015) in Eq. (3).

$$V_s(C) = \left(\frac{V_0}{1 + (C/X)^Q}\right), \tag{3}$$

where the fitting parameters $X$ [g/L] and $Q$ [-] govern the changes in magnitude of hindered settling with increasing solids concentration. It is instructive to compare the Takacs model with the explicit polydisperse sedimentation model of Masliyah (1979) (derived from first principles by Bürger et al., 2008), which characterises the sedimentation velocity $V_{(s,i)}$ of each particle class $i = 1 : N$ as

$$V_{(s,i)}(\mathbf{C}) = \frac{C_i}{\alpha_i(\mathbf{C})}(\rho_i - \rho(\mathbf{C}))g, \quad \text{for} \quad i = 1 : N. \tag{4}$$

Here $\mathbf{C} = (C_1, \cdots, C_N)$ is the vector of $N$ solids concentrations $C_i$ for each particle class $i = 1 : N$, $\rho_i$ is the density of the $i$th particle class, $\rho(\mathbf{C})$ is the volume-averaged suspension density (i.e. $\rho(\mathbf{C} = \sum_{i=1}^{N} C_i\rho_i + (1 - \sum_{i=1}^{N} C_i)\rho_f$, where $\rho_f$ is the fluid density), $g$ is gravitational acceleration, and $\alpha_i(\mathbf{C}$ quantifies viscous drag between the $i$th particle class and the fluid velocity. In practice, this drag term is very difficult to characterise for each particle class as it must be determined throughout the $N$-dimensional space $\mathbf{C}$ of all concentration combinations of all particle classes. To overcome this difficulty, Lockett and Bassoon (1979) propose the Richardson-Zaki (Richardson, 1954) functional form for the viscous drag coefficients as

$$\alpha_i(\mathbf{C}) = \frac{d_i^2}{18\mu_f} C_i (1 - C)^{n(\mathbf{C})-2} \quad \text{for} \quad i = 1 : N, \tag{5}$$

were $C = \sum_{i=1}^{N} C_i$ is the total solids fraction, $d_i$ is the diameter of particle class $i$, $\mu_f$ is the viscosity of the suspending fluid, and the index $n$ is a weak function of $\mathbf{C}$. Under the assumption $n = n(\mathbf{C})$ and uniform solids density $\rho_s$ across all particle classes (a reasonable assumption for waste water sludges), the settling velocity of each particle class simplifies to be solely a function of the total solids concentration $C$ as

$$V_{(s,i)}(C) = \frac{d_i^2\ g\left(\rho_s - \rho_f\right)}{18\mu_f}(1 - C)^{n-1} \quad \text{for} \quad i = 1 : N. \tag{6}$$

In a 1D batch settling model, the solids concentration field $C_i$ for each species is then described by the continuity equation

$$\frac{\partial C_i}{\partial t} + \frac{\partial}{\partial x}\left(C_i V_{(s,i)}(C)\right) = 0 \quad \text{for} \quad i = 1 : N. \tag{7}$$

Summing over all solids classes also yields a conservation equation for the total solids fraction:

$$\frac{\partial C}{\partial t} + \frac{\partial}{\partial x}\left[\sum_{i=1}^{N} C_i V_{(s,i)}(C)\right] = 0. \tag{8}$$

The Takacs model is similar to this polydisperse sedimentation model in that the sedimentation velocity of each particle class is solely a function of the total solids concentration $C$. The major difference is that the Takacs model does not resolve sedimentation of each particle class $i$, but rather lumps them all together into a single solids flux model

$$\frac{\partial C}{\partial t}+\frac{\partial}{\partial x}(C\overline{V}_s(C))=0,\quad \overline{V}_s(C)\approx\frac{1}{C}\sum_{i=1}^{N}C_iV_{(s,i)}(C). \tag{9}$$

Although the contribution of the non-settling fraction to this approximation is exact (as $V_{s,1}=0$), for the other fraction the total settling velocity $\overline{V}_s(C)$ is non-unique in that different distributions of particle fractions $C_i$ can yield the same total solids concentration $C$. However, if consideration is limited to sedimentation processes in a quiescent suspension (such as 1D batch sedimentation), it may be assumed that the distribution of $C_i$ can only vary to a limited degree for a given solids concentration. This is a reasonable approximation in regions where the local total solids concentration $C$ is less than or equal to the initial concentration $C_0$, as the fastest sedimenting particles settle out first, and so the solids distribution evolves in a unique manner. Conversely, $\mathbf{C}$ is not uniquely determined by $C$ in regions where $C>C_0$ as different particle classes $i$ can contribute to this increase in total solids as sedimentation proceeds (due to e.g. segregation at the interface of the supernatant and hindered zone). However, depending upon the particle size distribution, this variation may be limited in some systems. Furthermore, differential sedimentation ceases in the compression zone due to the formation of a contiguous solids matrix.

Thus the polydisperse nature of the suspension explains the non-monotone form of the sedimentation velocity profile in Eq. (2). In the dilute range, sedimentation velocity increases with solids concentration as more rapidly settling particles are present, whereas at higher solids concentrations this effect becomes less pronounced and hindered settling eventually takes over, reducing the sedimentation rate. It is important to note that the exponential functional form of the Takacs model does not necessarily mean that the sedimentation velocity profile $V_{(s,i)}(C)$ of each individual particle class is exponential, (indeed it may follow Eq. (5)), but rather this exponential form arises from the convolution of the sludge particle size distribution with $V_{(s,i)}(C)$.

Hence, while the Takacs model involves a number of assumptions and approximations that have not been extensively tested, it is closely related to *ab initio* models of polydisperse sedimentation and it does appear to capture the fundamental dynamics of these systems. Its continuous and smooth functional form Eq. (2) indicates that it applies to polydisperse suspensions with a continuous particle size distributions. The success of this model is that it can capture these complex dynamics in a simple model that only has a small number of fitting parameters, several of which have direct physical meaning. The major drawback of this model is that as the underlying approximations have not been extensively tested, it is difficult to determine limits of applicability of this model.

To impart some of the advantages on the Takacs model to the Vesilind and Diehl models, we apply the concept of a non-settling fraction $C_{\min}$ in the Takacs model to these models, such that the solids concentrations values $C$ in Eq. (1), and Eq. (3) is replaced by $(C-C_{\min})$, where settling velocity for any concentration below $C_{\min}$ is zero. That modification will make both Diehl and Vesilind describe the settling velocity in a bidisperse manner.

To provide compatibility with the CFD model, the solids concentrations $C$ values in all equations were converted to dimensionless solids volume fractions using the measured densities of both solids and liquor from the samples used. All models were modified to have an explicit solids volume fraction limit of 12 vol% to provide numerical stability at extremely high concentrations. This limit was determined based on operational observation in the lagoon to represent the highest practical concentration observed over years of operations.

### 2.3.3. Compression model

The compression model developed by Buscall and White (1987) and Bürger et al. (2005) (amongst many similar models in the literature) can be expressed in terms of the total solids volume fraction $\alpha_d$ as

$$\frac{\partial\alpha_d}{\partial t}=-\nabla\cdot\left(\alpha_d\overrightarrow{V_m}\right)-\nabla\cdot\left(\frac{\alpha_d\rho_c}{\rho_m}\overrightarrow{V_{hs}}\right)+\nabla\cdot\left(d_{comp}\nabla\alpha_d\right)+\nabla\cdot(\Gamma\nabla\alpha_d). \tag{10}$$

Where $\alpha_d$ is the solids volume fraction, $\alpha_{cr}$ is critical volume fraction (gel point) at which the solids phase forms a continuous network that can withstand and transmit stress, $\rho_c$ is the density of the continuous liquid phase, $\rho_d$ is the density of the dispersed solids phase, $\rho(\alpha)=\alpha\rho_s+(1-\alpha)\rho_f$ is the density of the solids and liquid mixture, $V_{hs}$ is the hindered settling velocity, and $\sigma_e^{'}$ is derivative of the effective solid stress as expressed in De Clercq et al. (2008). The compression term is,

$$d_{comp}=\begin{cases}0 & \text{when}\quad 0\le\alpha<\alpha_{cr},\\ \dfrac{\rho_d}{g(\rho_d-\rho_c)}V_{hs}(\alpha)\sigma_e^{'}(\alpha) & \text{when}\quad \alpha\ge\alpha_{cr}.\end{cases} \tag{11}$$

After converting all concentrations to dimensionless volume fraction the effective solid stress could be expressed as;

$$\sigma_e^{'}=\begin{cases}0 & \text{when}\quad 0\le\alpha<\alpha_{cr},\\ \dfrac{\lambda}{\beta+(\alpha_d-\alpha_{cr})*\rho_d} & \text{when}\quad \alpha\ge\alpha_{cr}.\end{cases} \tag{12}$$

Where units for $\lambda$ ($\mathrm{kgm^{-1}s^{-2}}$), $\beta$ ($\mathrm{kgm^{-3}}$), $\alpha_{cr}=C_{cr}/\rho_d$, and $\alpha_d$ represents the value of solids volume fraction (dispersed phase). For the full details on the development of the equations related to the compression model implemented see Valle Medina and Laurent (2020).

### 2.3.4. Geometry and meshing

The dilute and concentrated batch settling columns were cylindrical as described earlier. The Dilute settling column had cylindrical ports at the side used to take samples out at specific heights. In each case a 3D mesh was built using structured methodology (ANSYS ICEM advanced meshing), where all cylindrical shapes followed an O-grid topology to reduce maximum non-orthogonality (below 45°). Cell count for dilute and concentrated respectively was 263,749 and 242,688 hexahedral cells which are the counts that achieved mesh independence.

Additional 1D and 2D structured meshes were built for the same geometries to compare to the 3D simulations. The 1D mesh was a single column of 2000 hexahedral cells across the middle of the cylinder. The 2D mesh was a rectangular slice across the middle of each cylinder with 36,369 and 48,951 hexahedral orthogonal cells for dilute and concentrated respectively. Both the 1D and 2D meshes were independent at the mentioned cell count.

### 2.3.5. Boundary and initial conditions

All wall boundary conditions were set to no-slip for velocity, fixed flux pressure and zero gradient solids. In the experimental set for the dilute settling column, samples were drawn out of the system over time. This induced flow fields in the system and affected solids mass inside the column. The effect of sampling was considered in the 3D validation against experimental results, with one simplification that the top of the column in the 3D model displaces the removed volume with water at low inlet velocity to maintain the incompressible mass balance and avoid the need to include an air gap on the top boundary. The outlet ports were all included, and the measured volume withdrawn for samples was modelled as flow out of the settling column. Surface velocities at the top boundary were negligible and had no impact, but the volume lost had an impact that was evaluated and discussed in Section 3.1. In the 1D and 2D simulations, the boundaries were exactly the same, but replacing the removed spacial dimension with an empty boundary. The volume loss due to samples drawn out of the dilute settling column was not included in 1D/2D for comparison purpose.

### 2.3.6. Parameter optimisation and uncertainty quantification

A parameter sensitivity and optimisation process as identified in Section 2.2.1 was used, analysing firstly dilute tests using the three novel settling models, concentrated tests using the same models coupled with

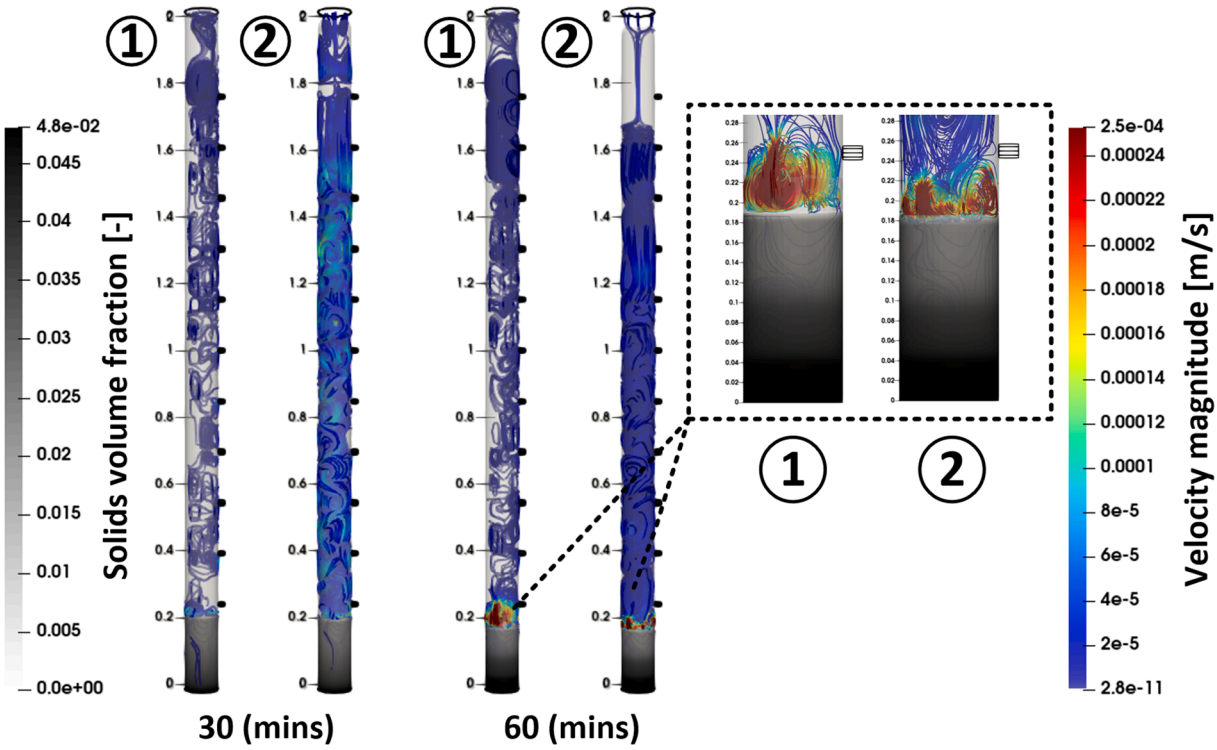


**Fig. 2.** 3D simulations of dilute batch settling column test starting from 5.76 g/L initial uniform solids concentration, (1) without accounting for samples drawn out, (2) accounts for samples lost volume.

compression, then assessing two combined models capable of simulating both dilute and concentrated ranges. Parameters values and correlated confidence regions were compared across all tests. In general, parameters were sampled broadly using Monte-Carlo techniques, and then at a high frequency around the optimum. Gradient and non-gradient search techniques were used to find actual optima, and the true confidence region was identified as noted below.

The uncertainty quantification studies were performed using a coupled process of three open source platforms (OpenFOAM, Dakota, and Python). Where OpenFOAM is the CFD simulation platform. Dakota provides the seeding, sampling, collection algorithm wrapping the CFD simulation. Python provides the numerical adjustment from OpenFOAM output to Dakota algorithm. The output from CFD simulation in case of the dilute batch settling is solids volume fraction at specific heights over time, which is edited and shaped by Python scripts to calculate RSS (Residual Sum of Squares) and then forwarded to collection algorithm to compile (Dakota). In case of the concentrated settling the CFD simulation output is solids volume fraction over vertical line (in the middle of the geometry) at each time step simulated. Python scripts process the output files, determine potential solids liquid interfaces from the vertical concentration derivative, and outputs the spatial interface from the maximum derivative. This results in a calculated SBH (Sludge bed height) at each time, which is compared to experimental results to calculate RSS. This value is forwarded to the collection algorithm to compile as in dilute case.

The selection and seeding algorithm used is LHS (Latin Hyper Cube), which is a randomised walk (Monte-Carlo) procedure. The compiled output is an objective function of RSS with regards to parameters sets. The studies in both cases were ran in series of 1000–2000 simulations blocks. In general, a coarse range of input parameter values was used in initial simulations to determine approximate optima, followed by a fine set of simulations to determine actual optima and confidence limits. The global minimum value of RSS is $J_{opt}$, and the value of $J_{crit}$ were determined by an F-distribution (Dochain and Vanrolleghem, 2001) test as in Eq. (13).

$$J_{crit} = J_{opt}\left(1 + \frac{p}{N_{data} - p} * F_{\alpha:p,N_{data}-p}\right). \tag{13}$$

Where $J_{opt}$ is the minimum value found for the objective function (Residual Sum of Squares) and $F_{\alpha:p,N_{data}-p}$ is the value of F-distribution with $p$ and $N_{data} - p$ degrees of freedom and a confidence level $\alpha$ (95%).

For final optimization, $J_{opt}$ from the uncertainty study was checked using a derivative free DIRECT method (Dividing Rectangles) to find global optima with wide bounds. This was followed by a Newton optimisation to confirm convergence to the local optima. The results were compared to confirm the uncertainty study findings or correct $J_{opt}$ if found to be different.

### 2.3.7. Pilot continuous simulations

The pilot shown in (Fig. 8) is 2 m long, 0.5 m wide, 0.3 m high at the inlet side, 0.4 m high at outlet side, bottom is sloped at 1:10, inlet pipe diameter is 0.1 m, and underflow is a centralised square outlet with edge length of 0.1 m.

Following a typical primary settling tank design, the flow rate of the underflow is 1/20 to the inlet flow rate. The pilot was simulated at three set of inlet flow rates; 5.9 L/min, 29.4 L/min, and 58.8 L/min with the underflow adjusted accordingly. The simulation time for the mentioned flow rates was 48, 12, and 6 h respectively, which is 24–48 times the HRT (Hydraulic Retention Time) in each case. Pilot total volume is 0.3525 $m^3$ and HRT value at the lowest flow rate is 1 h.

The mesh built for the geometry is structured fully hexahedral with a cell count of 850,976 based on the mesh Independence test. For the boundary and initial conditions, the inlet and underflow were set to flow rate controlled, and the outlet over flow weir was set to free flow out. The starting sludge bed height was 10% of the total height with uniform solids volume fraction of 3.5%, and the inlet solids volume fraction was 0.1% the equivalent of 1 g/L.

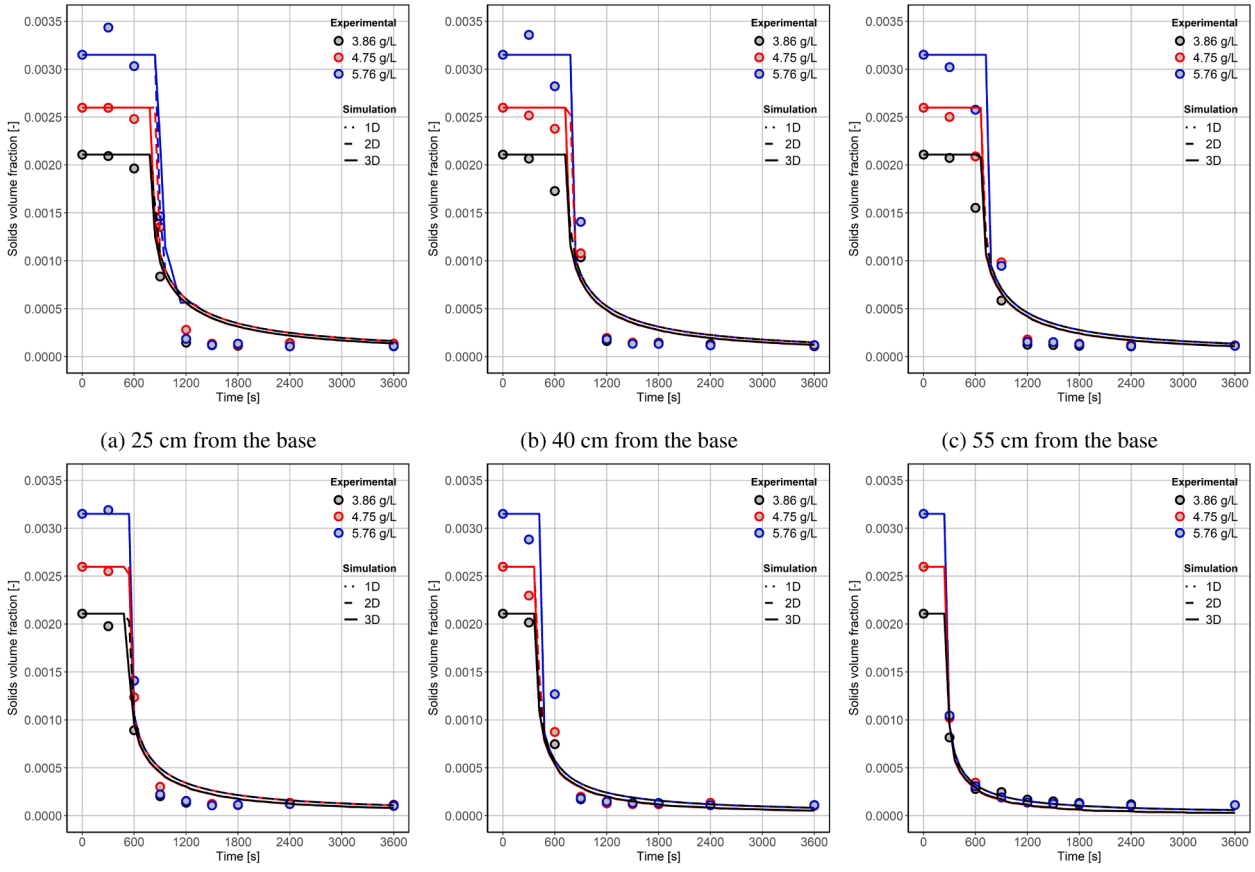


(a) 25 cm from the base (b) 40 cm from the base (c) 55 cm from the base

(d) 85 cm from the base (e) 115 cm from the base (f) 145 cm from the base

**Fig. 3.** 1D/2D/3D modelling of dilute settling starting from uniform concentrations ranging 3–6 g/L using Takacs model compared to experimental results, 3D simulations took into account volume loss due to samples and turbulence, while 1D/2D simulations did not.

**Table 1**
Optimized parameters and sum of RSS for Takacs, Vesilind, and Diehl models compared to dilute batch settling column experimental test.

| Model | $V_0$ [m/s] | $R_h$ [-] | $R_p$ [-] | $X$ [-] | $Q$ [-] | RSS [-] |
|---|---|---|---|---|---|---|
| Takacs | $3.01 \times 10^{-3}$ | 128.7 | 725.7 | - | - | $5.14 \times 10^{-6}$ |
| Diehl | $1.94 \times 10^{-3}$ | - | - | 0.26 | 7.05 | $1.67 \times 10^{-5}$ |
| Vesilind | $2.13 \times 10^{-3}$ | 29.54 | - | - | - | $2.27 \times 10^{-5}$ |

## 3. Results and discussion

### 3.1. Dilute settling column sampling effect

Samples drawn during the dilute settling column did reduce the mass of solids inside the domain. This resulted in a 10 mm sludge bed height difference between the two 3D simulations with and without samples (Fig. 2), as well as minor differences at the top of the column. However, differences in solid phase velocities, and hence concentration profiles between 3D with sampling, 3D without sampling and 1/2D were negligible (Fig. 3). This was mainly because of the low initial concentrations and the overall low velocity profiles. The 3D vs 1/2D as shown in Fig. 3 also indicates negligible impacts of turbulence and boundary effects. This shows approximately 5% deviation for 1D and almost identical 2D and 3D results. Since the sludge bed height is not the focus of this test, the 1D/2D models without sampling may be used used for optimization and uncertainty analysis.

### 3.2. Dilute settling column simulations

As noted in methods, the three initial conditions (assumed to be uniform) were 3.86 g/L, 4.75 g/L, and 5.76 g/L). Each of the initial conditions was optimised separately using each model (to check these values). The total residual sum of squares and optimised parameters for the three models are combined and detailed in (Table 1). Notably, the Takacs sum of residuals is one order of magnitude less than both Diehl and Vesilind, representing a significantly better model. Therefore only uncertainty analysis for the Takacs model is presented here. In terms of simulations required, DIRECT optimization required 150–200 iterations, Newton optimization required 20 iterations, and additional parameter sampling to identify confidence regions was 6000 simulations.

The effect of non uniform initial concentrations in the experiment could be observed from (Fig. 3a) and (b) at 300 and 600 sec leading to deviation. The downward deviation could be a results of the same non uniform initial condition or alternatively due to polydispersed behaviour not captured by the optimised model. The relatively large size of the column added to non-uniform initial conditions. However, unless a non-intrusive accurate method of measuring the solids concentration is used, a larger volume is necessary to draw sufficient samples without having a significant impact on the sedimentation behaviour. Additionally the simulation outlet boundary condition needs to take into account the hydrostatic pressure difference between the higher and lower ports, which will lead to more solids drawn out from lower ports. Such measure could not be captured accurately in CFD, unless an air phase is introduced to the model, where the water column inside the simulation will decrease with time and take into account that effect.

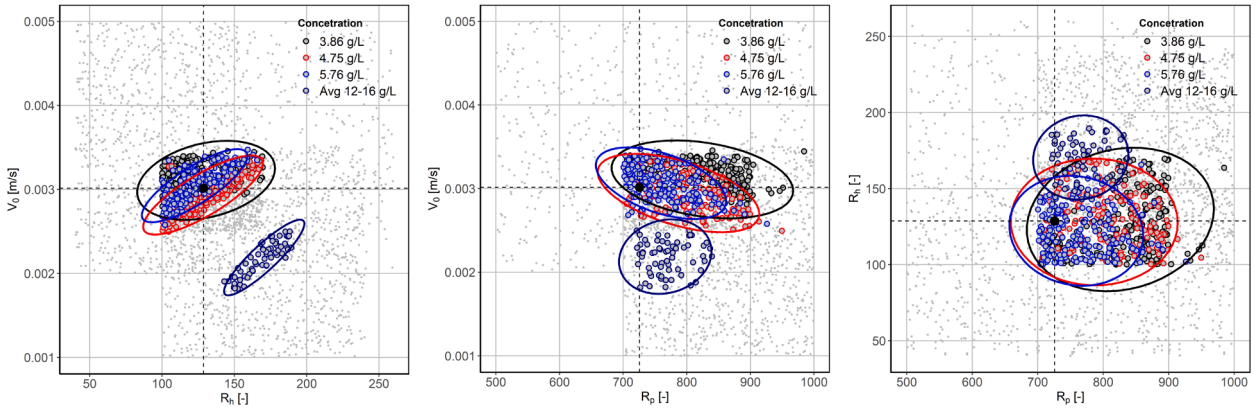


(a) $R_h$-$V_0$ confidence regions (b) $R_p$-$V_0$ confidence regions (c) $R_p$-$R_h$ confidence regions

**Fig. 4.** Takacs model parameters 95% confidence interval regions and correlation, the gray points in the background represent all final stages simulated parameters, the black point with cross dotted lines is the optimum values, the highlighted colored points are the simulated parameters that resulted in $J < J_{crit}$, and the ellipses are the interpolated 95% confidence for each concentration separately.

**Table 2**
Optimized parameters and sum of RSS for continuous function models when coupled with compression models compared to the results of concentrated batch settling experimental tests.

| Model | $V_0$ [m/s] | $R_h$ [-] | $R_p$ [-] | $X$ [-] | $Q$ [-] | $\beta$ [$kgm^{-3}$] | $\lambda$ [$kgm^{-1}s^{-2}$] | $\alpha_{cr}$ [-] | RSS [-] |
|---|---|---|---|---|---|---|---|---|---|
| TC (Conc. opt.) | $1.82 \times 10^{-3}$ | 152.37 | 726.98 | - | - | 0.788 | 6.421 | 0.020 | $1.20 \times 10^{-3}$ |
| DC (Conc. opt.) | $0.54 \times 10^{-3}$ | - | - | 0.017 | 7.69 | 0.798 | 5.869 | 0.018 | $3.28 \times 10^{-3}$ |
| VC (Conc. opt.) | $3.22 \times 10^{-3}$ | 212.94 | - | - | - | 0.305 | 5.271 | 0.023 | $1.13 \times 10^{-3}$ |
| TC (Dilute opt.) | $3.01 \times 10^{-3}$ | 128.73 | 725.71 | - | - | 0.840 | 6.069 | 0.016 | $2.64 \times 10^{-2}$ |

The 95% confidence regions for parameters from the dilute tests are shown in (Fig. 4) for each concentration together with correlated ellipses. Also shown is the region identified from the concentrated batch settling uncertainty studies for two concentrations between 12–16 g/L (Section 3.3). As can be seen, the three regions overlap, with moderate uncertainty ranges (20%). $V_0$ had the highest sensitivity followed by $R_h$ while $R_p$ had the lowest sensitivity. From (Fig. 4b) a positive correlation is present between $V_0$ and $R_h$, and a weak negative correlation between $V_0$ and $R_p$ in (Fig. 4c). Overlap of the three dilute tests indicate that the solids behave consistently in this range (4–6 g/L). As noted, $V_0$ decreased significantly in the concentrated batch settling tests, while the $R_h$ and $R_p$ ranges overlapped, indicating that the material is behaving consistently at 12–16 g/L, but with a decreased velocity. It is interesting that both $R_h$ and $R_p$ can be identified and are consistent across the fairly broad range of concentrations.

The 12–16 g/L confidence region results from the same uncertainty study based on the concentrated batch settling also shown in (Fig. 4). The plotted region is the result of combining Takacs with compression model (TC) and optimizing all parameters for both components against the concentrated batch settling experimental tests. That means that range is the optimum 95% confidence region of the concentrated settling behaviour for the same sludge. If the regions did overlap between dilute and concentrated, the behaviour could be modelled with a high degree of accuracy using one settling function and compression model. However, that non-overlap means optimizing the concentrated solids range will lead to increased errors in dilute solids range and vice versa.

### 3.3. Concentrated batch settling simulations

#### 3.3.1. Continuous function models

The two higher concentration tests in lab-scale cylinders were numerically simulated for 4 h, each measuring solids interface over time. Using the same methodology, all three models (Vesilind, Takacs, Diehl) were optimised (for all parameters - sedimentation and compression) when coupled with the compression model. From values in (Table 2), the RSS is similar for all three models. The sludge bed height over time plots were almost identical and demonstrate they are functionally the same. $V_0$ consistently dropped with all three models, which suggests that a further decrease in $V_0$ is required, in addition to the compression, to describe the increase in hindered behaviour as solids concentration increases towards the compression zone. The uncertainty quantification studies were performed over 6000 simulations for TC (Takacs and Compression model), and 4000 simulations for each of VC and DC (Vesilind/Diehl and Compression model). The optimisation using DIRECT and Newton methodology required 200–250 iterations combined for each model. To visualise the difference due to the significant drop in $V_0$ compared to dilute optimum parameters, the Takacs model dilute 95% CI range was plotted against the Takacs-compression 95% CI range in (Fig. 4). The clear separation in confidence regions in (Fig. 4a) shows that if the dilute parameters (3–6 g/L) are fixed to optimum, while only compression parameters in Eq. (12) are optimised to fit the experimental data, the RSS in concentrated range rises by one order of magnitude (Table 2) and the visual fit is poor (Fig. 6).

To further assess whether the apparent difference in $V_0$ was due to compression or hindering, Takacs parameters were set to the optimum from (Table 1), and only compression parameters modified. The optimum values shown in (Table 2) (TC Dilute opt.) identify the compression model attempting to address deviations by raising the value of $\alpha_{cr}$ to reduce the settling velocity. However, the optimal RSS is an order of magnitude compared to (TC Conc. Opt.). When done in reverse and focused on Concentrated only, the RSS in Dilute increased by two orders of magnitude. These results indicate a simple global Takacs model is not suitable for wide solids concentration ranges, even when coupled with compression model. While it is necessary to maintain a simple practical model, it is also necessary to maintain an acceptable level of accuracy. The practical implications of this are further discussed below.

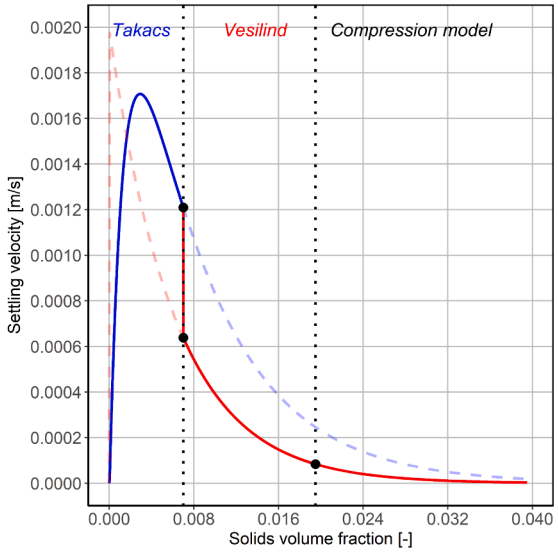


**Fig. 5.** TVC combined model settling velocity as function of solids volume fraction using optimized parameters from this study.

### 3.3.2. *Combined function models*

This section assesses combination of two settling models with compression following the same concept in Ramin et al. (2014). The first combined model is referred to as TDC (Takacs, Diehl and Compression model), which utilises Takacs for dilute, Diehl above the switch value and compression. That is, Eq. (2) applies at concentrations lower than the switch, and Eq. (3) above the switch, incorporating compression. The second combined model is TVC (Takacs, Vesilind, and Compression), with Eq. (2) at concentrations below the switch, and Eq. (1) above the switch as shown in (Fig. 5). The value of $C_{switch}$ has been optimized to be (0.7 vol%) solids volume fraction.

The Takacs model in both cases has the three optimal parameters taken from dilute settling tests in Section 3.2. The TDC has an additional 6 parameters to describe the concentrated range ($V_2$, $X$, $Q$, $\alpha_{cr}$, $\beta$, $\lambda$), while the TVC model has an additional 5 parameters ($V_2$, $R_v$, $\alpha_{cr}$, $\beta$, $\lambda$). These additional parameters were optimised using the concentrated tests (12.71 and 15.58 g/L). The optimised RSS for the TDC function was ($2.944 \times 10^{-3}$) whereas for the TVC function it was ($9.575 \times 10^{-4}$). TDC optimised parameters are shown in (Table 3), while TVC optimised parameters are shown in (Table 4). As shown in (Fig. 6), The two models are not functionally different (and similar in 1-3D). While Diehl (TDC) can adequately represent both concentrations, it has one additional parameter compared to Vesilind, and overall, a higher RSS (poorer fit), indicating a poorer model overall. Optimising compression parameters only for Takacs does not allow an acceptable fit.

While we used a switch as well as an explicit Vesilind function for the concentrated regime, it is noted that at high concentration, Vesilind and Takacs models are functionally identical, and it would be possible to further simplify the model by utilising Takacs across the whole con-

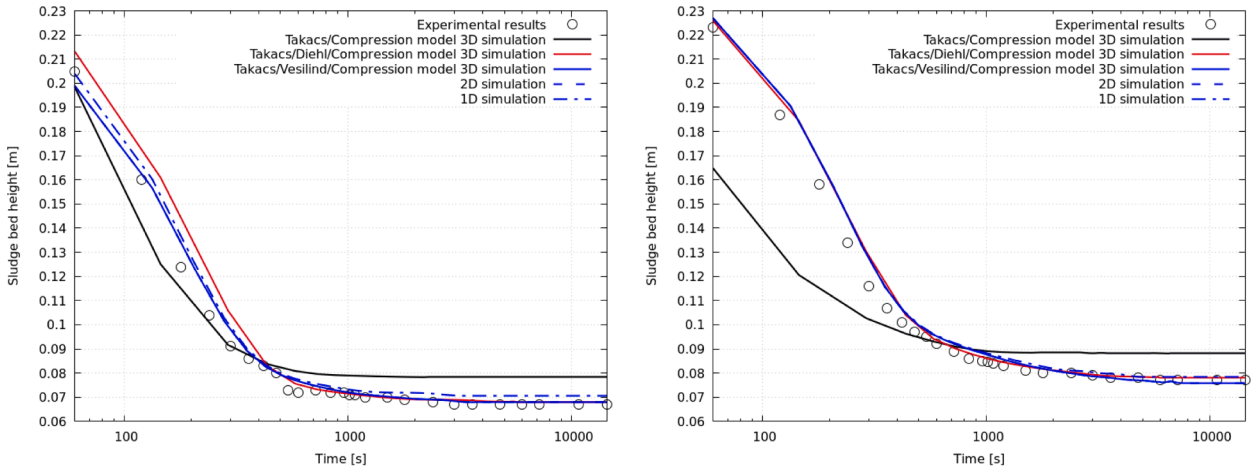


(a) Uniform 12.71 g/L initial condition

(b) Uniform 15.58 g/L initial condition

**Fig. 6.** 3D simulation of concentrated batch settling starting from two different uniform solids concentration using three models at their optimised parameters, comparing 1D and 2D simulations results to 3D simulations using TVC model.

**Table 3**
TDC combined model optimized parameters and 95% confidence interval range compared to concentrated batch settling experimental test results.

| Parameter | $V_1$ [m/s] | $R_h$ [-] | $R_p$ [-] | $V_2$ [m/s] | $X$ [-] | $Q$ [-] | $\alpha_{cr}$ [-] | $\beta$ [kgm$^{-3}$] | $\lambda$ [kgm$^{-1}$s$^{-2}$] |
|---|---|---|---|---|---|---|---|---|---|
| Optimum value | $3.014 \times 10^{-3}$ | 128.7 | 725.7 | $5.119 \times 10^{-4}$ | 0.017 | 5.827 | 0.021 | 0.735 | 7.570 |
| Lower 95% CI range | $2.5 \times 10^{-3}$ | 100 | 700 | $4.619 \times 10^{-4}$ | 0.012 | 4.007 | 0.020 | 0.415 | 7.006 |
| Higher 95% CI range | $3.5 \times 10^{-3}$ | 150 | 850 | $5.995 \times 10^{-4}$ | 0.020 | 7.906 | 0.022 | 0.799 | 7.942 |

**Table 4**
TVC combined model optimized parameters and 95% confidence interval range compared to concentrated batch settling experimental test results.

| Parameter | $V_1$ [m/s] | $R_h$ [-] | $R_p$ [-] | $V_2$ [m/s] | $R_v$ [-] | $\alpha_{cr}$ [-] | $\beta$ [kgm$^{-3}$] | $\lambda$ [kgm$^{-1}$s$^{-2}$] |
|---|---|---|---|---|---|---|---|---|
| Optimum value | $3.014 \times 10^{-3}$ | 128.7 | 725.7 | $1.982 \times 10^{-3}$ | 162.5 | 0.019 | 0.896 | 6.175 |
| Lower 95% CI range | $2.5 \times 10^{-3}$ | 100 | 700 | $1.606 \times 10^{-3}$ | 139.9 | 0.019 | 0.637 | 6.008 |
| Higher 95% CI range | $3.5 \times 10^{-3}$ | 150 | 850 | $2.043 \times 10^{-3}$ | 169.0 | 0.020 | 0.910 | 6.618 |

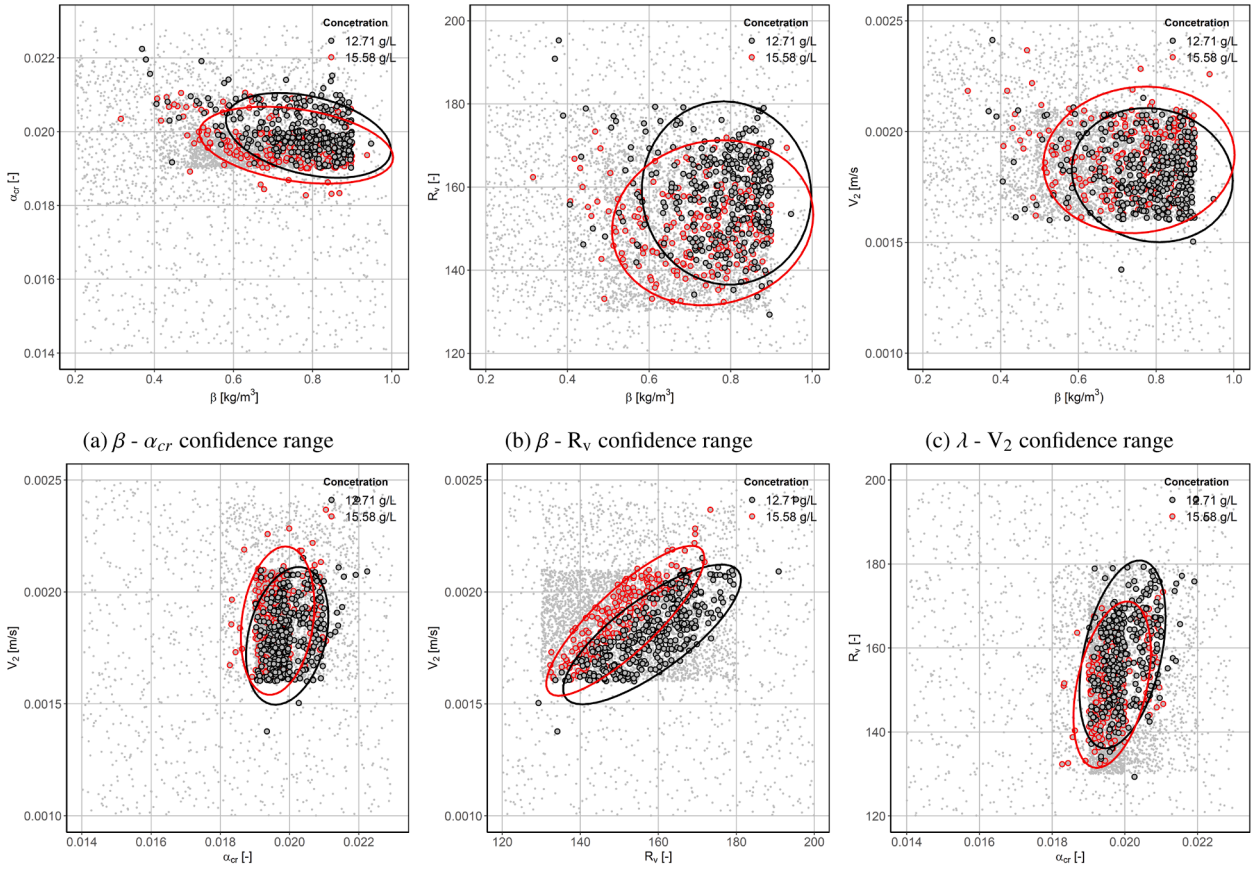


(a) $\beta$ - $\alpha_{cr}$ confidence range (b) $\beta$ - $R_v$ confidence range (c) $\lambda$ - $V_2$ confidence range

(d) $\alpha_{cr}$ - $V_2$ confidence range (e) $R_v$ - $V_2$ confidence range (f) $\alpha_{cr}$ - $R_v$ confidence range

**Fig. 7.** TVC combined model parameters 95% confidence interval regions and correlation.

centration domain, and only switching $V_0$ to its lower optimum of 0.0021 above the switch concentration. This would eliminate $R_v$, since it is effectively replaced by $R_h$. Note that the confidence intervals for $R_h$ and $R_v$ overlap and adjusting $R_v$ would change $V_2$ to the above value (Fig. 7e). This reduces the concentrated range number of parameters to 4 ($V_0$ as well as the three compression parameters).

Confidence regions for both concentrations are shown in (Fig. 7). This indicates generally a low degree of correlation particularly between compression parameters (indicating they are identifiable and independent), and only substantial correlation between the hindered settling parameters ($V_2$ and $R_v$), which is discussed above. The total count of 2D simulations performed in both uncertainty quantification studies for the two mentioned combined models is 24,000 Simulations, following the same methodology mentioned in Section 2.2.1 and Section 2.3.6.

### 3.4. Transient 3D simulations

To display the differences between the compared models combination, and the optimization/calibration process effects on practical industrial application, we created a test primary pilot settling tank geometry shown in (Fig. 8). The turbulence model used was LES (Smagorinsky, 1963). The rheology model was fitted for the sludge as solids volume fraction dependent combined power law and Herschel Bulkley. All models and conditions were fixed through all simulations except for the settling models used. The settling models simulated and compared are TC(Conc. opt.), TC(Dilute. opt.), and TVC with their respective optimized parameters.

The model comparison is based on the key performance metrics of solids capture, average solids out, and the sludge bed profile at the end of each simulation. Solids capture was calculated by averaging solids from the underflow divided by the solids in during the last hour of each simulation, which was consistently close to quasi steady-state convergence.

Calculated solids capture is shown in (Table 5) for each simulation with the respective model used, using the TVC model as a benchmark, the errors in each case is highlighted in red when the comparison model is low compared to reference model, and blue when it is high. The results are consistent with the analysis performed showing that optimization with bias toward either low or high concentration range is inaccurate compared to the reference model. Furthermore, depending on the dynamic condition of the simulation/process the errors are magnified with an oscillation range between 12.39% underestimation to 17.97% overestimation. When the same case was simulated using Takacs model alone, it became numerically unstable after few hours. The reason for this is as there is no compression model attached, solids settled too fast, accumulating at the bottom of the pilot until reaching the packing limit. Because the rheology model is solids concentration dependent, the sludge bed of 12% vol has a very high viscosity and does not move. That either leads to a simulation that does not represent reasonable physical behaviour, or numerical instability due to high gradients.

Furthermore, when contours from the side view are visualised through a slice across the middle of the pilot (Fig. 9), the differences between the three models are marginal, but with observable differences in sludge profile. However the resulting top view sludge bed profiles over time in all 3 cases were noticeably different as shown in (Fig. 10). Specifically the scoured sludge bed portion being substantially different for the dilute TC at higher flow rates. The TC(dilute opt.) model usually resulted in more and faster washout compared to the other two models. Videos of simulation contours development and 3D volume rendering of velocity magnitude/solids volume fraction over time for all three models

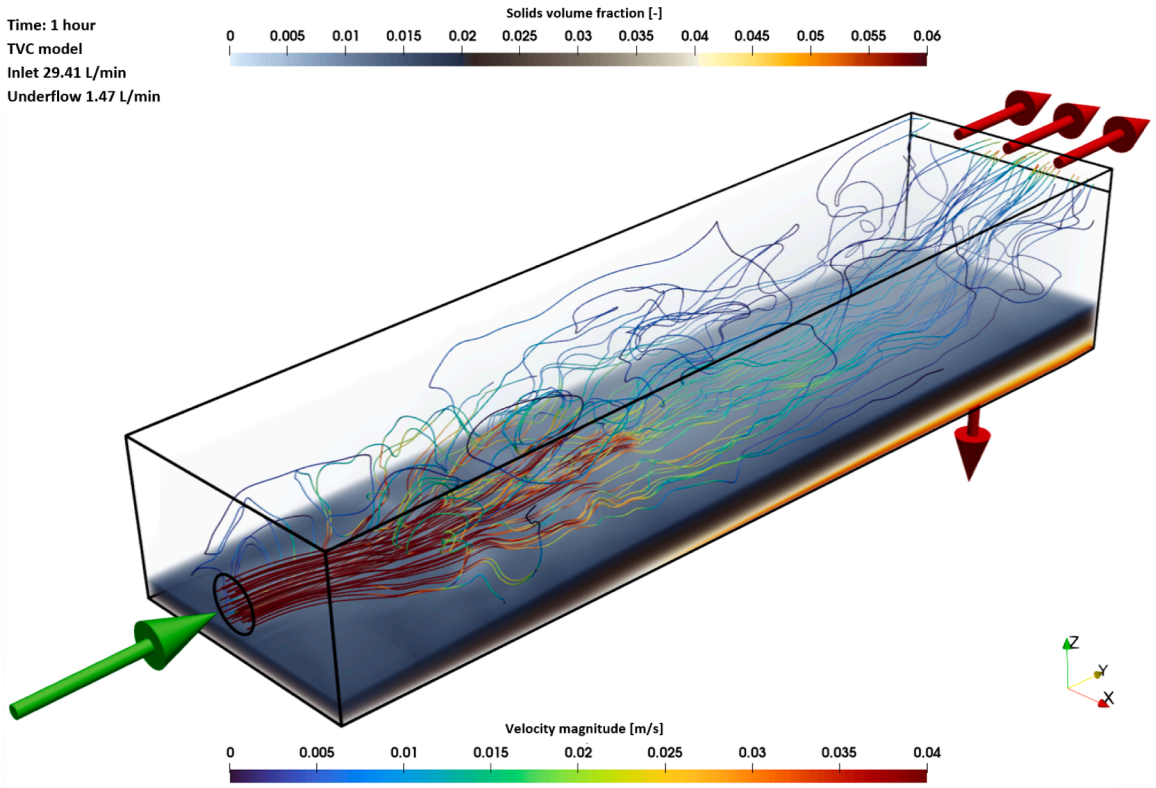


**Fig. 8.** Primary pilot settling tank simulation using TVC model at four hours, volume rendered solids volume fraction and velocity streamline.

**Table 5**
Solids capture calculated from the last hour of each transient 3D simulation of the primary pilot using different combinations of sedimentation models and several flow rates.

| | Values | | |
|---|---|---|---|
| $Q_{inlet}$ [L/min] | 5.88 | 29.38 | 58.75 |
| $Q_{underflow}$ [L/min] | 0.294 | 1.469 | 2.938 |
| TVC model solids capture | 80.67% | 75.42% | 35.58% |
| TC model (Dilute. opt.) | 98.64% | 85.96% | 37.55% |
| solids capture | (+17.97%) | (+10.54%) | (+1.97%) |
| TC model (Conc. opt.) | 85.24% | 74.56% | 23.19% |
| solids capture | (+4.57%) | (-0.86%) | (-12.39%) |

is provided in the data repository associated with this paper (Abood, 2022b). This includes underload simulation results (5.88 L/min), normal load simulation results (29.38 L/min), and Overload simulation results (58.74 L/min). The full raw data for computational work involved could be found in the following data repository (Abood, 2022a).

### 3.5. Analysis

1D,2D, and 3D simulations for experimental tests were effectively the same with minor differences. The same applies for samples withdrawn from the dilute batch settling having marginal influence. Polydisperse sludge with relatively high solids concentration range sedimentation could be effectively modelled with empirical functions, but require additional considerations, and either modification from single function models to multiple models (across different ranges), or change in the key parameter of maximum sedimentation velocity. As seen in this paper, the change can be relatively minor (i.e., change in a single parameter).

The requirement to incorporate differential behaviour at high/low range is particularly important if concentration dependant rheology models are used, which will result in not an only poor prediction, but also numerical instability at high concentrations, resulting from over-

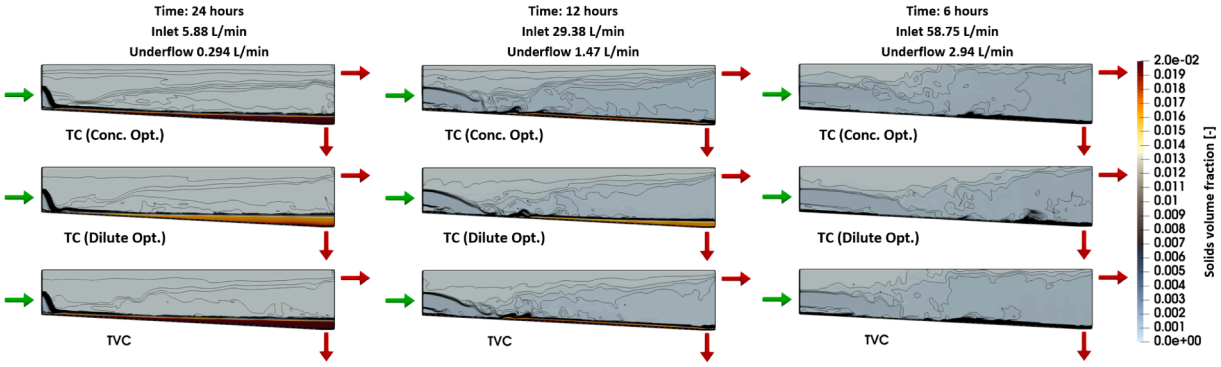


**Fig. 9.** Side view of primary pilot tank with plotted sludge bed contours for each model at simulation end using different flow rates.

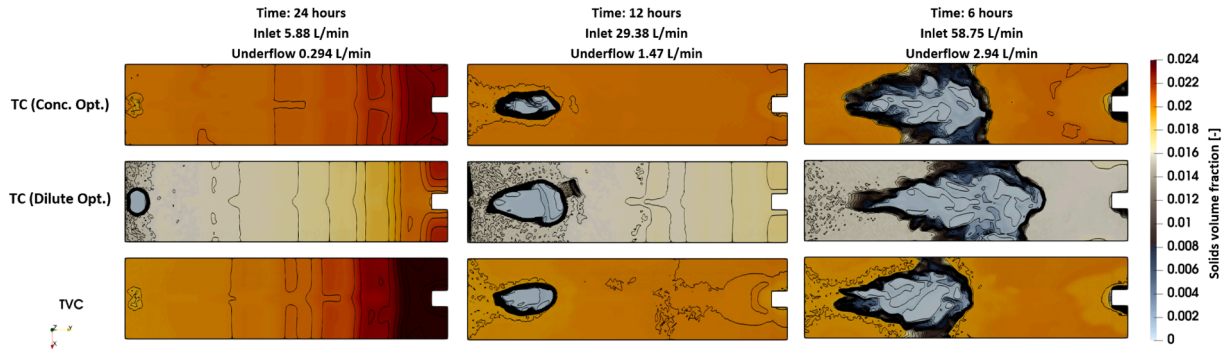


**Fig. 10.** Top view of primary pilot tank with plotted sludge bed contours for each model at simulation end using different flow rates.

sedimentation. This was observed in the continuous flow example assessed here. Single function models can be effectively fit to a single test, but tests in multiple ranges and with different measurement methods expose the differential behaviour. The inclusion of uncertainty analysis is critical, and relatively low cost (computationally) if applied in 1D or 2D model simulations.

The differences between such combined approach and simpler forms evaluated here were magnified in a dynamic environment and larger scale, especially when increasing flow rates or under washout/failure conditions (Such as wet weather events or overloading in industrial applications). That implies an even higher effect on larger industrial systems, and provides some indication of why it has been classically difficult to model polydispersed material in primary settling tanks and anaerobic lagoons simulations in the limited literature cases (Brennan, 2001; Dahl, 1995; Liu and García, 2011; Samstag et al., 2016).

On the experimental side, testing improvements are clearly needed. A wider range of solids concentration should be included in the testing and optimization. Minimizing interference is also a priority, or preferably a non-intrusive measurement method that could work accurately in both low and high solids concentrations. Repeatable experimental tests are also necessary to establish error analysis for experimental measurements and provide higher certainty, though these tests are labor intensive (particularly dilute settling tests). In general, it is better to replicate tests rather than collect more samples in a given test.

The results also indicated that for simple tests, multi-dimensional analysis is not required. We used HPC resources (High Performance Computing), but this is not necessary for 1D uncertainty analysis. 1D-3D had consistent results, but computational costs varied substantially. The grid considered 2000 cells for 1D, 49,000 cells for 2D, and 260,000 cells for 3D. Considering an HPC service unit (SU) is 1 core x 1 h, the 1D case required 0.1 SU/simulation, 2D required 3 SU/simulation, and 3D required 26 SU/simulation. Therefore, while 2D and 3D cases can be modelled on workstations, uncertainty analysis can only be done in 1D. To perform uncertainty analysis in 2D and 3D, HPC solution is required. Note that the estimated computational cost calculations are based on the approximate cost of $A0.07/SU, which might vary between different HPC solutions providers. The total computational cost of all uncertainty analysis included in this work performed in 2D cost approximately $A6448, which is 87% less than the estimated cost of conducting the same simulations in 3D approximately $A51880. We recommend that uncertainty analysis on parameters also be applied to continuous flow systems (which are best analysed in 2-3D), and this obligately requires HPC resources, but 2D results is an order of magnitude cost reduction vs 3D analysis. For reference, simulation for one of the 3D continuous flow examples used here under the lowest flow rate condition required 5 KSU.

## 4. Conclusion

Analysis of polydispersed batch sedimentation at both low (3–6 g/L) and high (12–16 g/L) initial concentrations indicated that the Takacs model was the most effective at low concentration range, while at high concentration ranges, all models performed similarly when coupled with a compression model. Comparing individual parameter sets across both domains identified no changes to hindered parameters ($R_h$, $R_p$), but that the effective $V_0$ decreased by approximately 50% from low to high concentrations even with a compression model coupled. This could be included via a switch function which enabled change to a different model, or reduction of V0 at elevated concentrations.

Analysis in a continuous flow-through primary sedimentation indicated that use of dilute parameters caused deviation under normal and underload conditions, while use of concentrated parameters caused deviation under overload conditions. While this study validates the general use of the Takacs model for polydispersed materials such as primary sludge and digestate, compression implementation is critical, and wide concentration range experimental testing coupled with uncertainty quantification is required to adopt such a combined model approach.

## Declaration of Competing Interest

The authors declare that they have no known competing financial interests or personal relationships that could have appeared to influence the work reported in this paper.

## Acknowledgements

This research was supported by the Australian Government through the Australian Research Council's Linkage Projects funding scheme (project LP170100257). We also acknowledge provision of computing resources and services from the Research Computing Centre (RCC) supported by the University of Queensland, and National Computational Infrastructure (NCI), which is supported by the Australian Government. Infrastructure support at The University of Melbourne was partially provided by the ARC Centre of Excellence for Enabling Eco-Efficient Beneficiation of Minerals (grant number CE200100009). Support of the Melbourne Water Corporation providing materials and samples is acknowledged.

## References

Abood, K., 2022a. [Dataset] characterising sedimentation velocity of primary wastewater solids and effluents [raw data]. https://doi.org/10.48610/34458e8.
Abood, K., 2022b. [Dataset] transient 3D simulations of three optimized sedimentation models using open source CFD drift-flux solver in OpenFOAM (low, high and normal flowrate). https://doi.org/10.48610/805a8a0.
APHA, 2005. Standard Methods for the Examination of Water and Wastewater. American Public Health Association, Washington DC.
Batchelor, G., 1972. Sedimentation in a dilute dispersion of spheres. J. Fluid Mech. 52 (2), 245–268.
Batchelor, G., 1977. The effect of Brownian motion on the bulk stress in a suspension of spherical particles. J. Fluid Mech. 83 (1), 97–117.
Batchelor, G., 1982. Sedimentation in a dilute polydisperse system of interacting spheres. Part 1. General theory. J. Fluid Mech. 119, 379–408.

Batchelor, G., Van Rensburg, R.J., 1986. Structure formation in bidisperse sedimentation. J. Fluid Mech. 166, 379–407.
Brennan, D., 2001. The numerical simulation of two phase flows in settling tanks. Imperial College London (University of London). Ph.D. thesis.
Bürger, R., 2000. Phenomenological foundation and mathematical theory of sedimentation–consolidation processes. Chem. Eng. J. 80 (1–3), 177–188.
Bürger, R., Diehl, S., Nopens, I., 2011. A consistent modelling methodology for secondary settling tanks in wastewater treatment. Water Res. 45 (6), 2247–2260.
Bürger, R., Garcia, A., Kunik, M., 2008. A generalized kinetic model of sedimentation of polydisperse suspensions with a continuous particle size distribution. Math. Models Methods Appl. Sci. 18 (10), 1741–1785.
Bürger, R., Karlsen, K.H., Tory, E.M., Wendland, W.L., 2002. Model equations and instability regions for the sedimentation of polydisperse suspensions of spheres. ZAMM 82 (10), 699–722.
Bürger, R., Karlsen, K.H., Towers, J.D., 2005. A model of continuous sedimentation of flocculated suspensions in clarifier-thickener units. SIAM J. Appl. Math. 65 (3), 882–940.
Buscall, R., White, L.R., 1987. The consolidation of concentrated suspensions. Part 1.-The theory of sedimentation. J. Chem. Soc., Faraday Trans. 1 83 (3), 873–891.
Cole, R.F., 1968. Experimental evaluation of the Kynch theory. University of North Carolina at Chapel Hill. Ph.D. thesis.
Dahl, C.P., 1995. Numerical Modelling of Flow and Settling in Secondary Settling Tanks. Series paper No. 8. Hydraulics and Coastal Engineering Laboratory, Department of Civil Engineering, Aalborg University.
De Clercq, J., Nopens, I., Defrancq, J., Vanrolleghem, P.A., 2008. Extending and calibrating a mechanistic hindered and compression settling model for activated sludge using in-depth batch experiments. Water Res. 42 (3), 781–791.
Diehl, S., 2007. Estimation of the batch-settling flux function for an ideal suspension from only two experiments. Chem. Eng. Sci. 62 (17), 4589–4601.
Diehl, S., 2015. Numerical identification of constitutive functions in scalar nonlinear convection-diffusion equations with application to batch sedimentation. Appl. Numer. Math. 95, 154–172.
Dochain, D., Vanrolleghem, P.A., 2001. Dynamical Modelling & Estimation in Wastewater Treatment Processes. IWA publishing.
Eshtiaghi, N., Markis, F., Yap, S.D., Baudez, J.-C., Slatter, P., 2013. Rheological characterisation of municipal sludge: a review. Water Res. 47 (15), 5493–5510.
Gernaey, K., Vanrolleghem, P., Lessard, P., 2001. Modeling of a reactive primary clarifier. Water Sci. Technol. 43 (7), 73–81.
Griborio, A., McCorquodale, J.A., Rodriguez, J.A., 2014. CFD modeling of primary clarifiers: the state-of-the-art. Proc. Water Environ. Fed. 2014 (8), 1926–1949.
Griborio, A., Valle-Medina, M., Laurent, J., Samstag, R., Wicks, J., Nopens, I., 2022. Chapter 6 - Sedimentation in CFD Modelling for Wastewater Treatment Processes. IWA Publishing, London.
Guazzelli, E., Hinch, J., 2011. Fluctuations and instability in sedimentation. Annu. Rev. Fluid Mech. 43, 97–116.
Hinch, E., 1977. An averaged-equation approach to particle interactions in a fluid suspension. J. Fluid Mech. 83 (4), 695–720.
Kynch, G.J., 1952. A theory of sedimentation. Trans. Faraday Soc. 48, 166–176.
Lakehal, D., Krebs, P., Krijgsman, J., Rodi, W., 1999. Computing shear flow and sludge blanket in secondary clarifiers. J. Hydraul. Eng. 125 (3), 253–262.
Lester, D.R., Usher, S.P., Scales, P.J., 2005. Estimation of the hindered settling function R ($\phi$) from batch-settling tests. AlChE J. 51 (4), 1158–1168.
Liu, X., García, M.H., 2011. Computational fluid dynamics modeling for the design of large primary settling tanks. J. Hydraul. Eng. 137 (3), 343–355.
Lockett, M.J., Bassoon, K., 1979. Sedimentation of binary particle mixtures. Powder Technol. 24 (1), 1–7.
Masliyah, J.H., 1979. ]Hindered settling in a multi-species particle system. Chem. Eng. Sci. 34 (9), 1166–1168.
Nguyen, N.-Q., Ladd, A.J., 2005. Sedimentation of hard-sphere suspensions at low Reynolds number. J. Fluid Mech. 525, 73–104.
Plósz, B.G., Weiss, M., Printemps, C., Essemiani, K., Meinhold, J., 2007. One-dimensional modelling of the secondary clarifier-factors affecting simulation in the clarification zone and the assessment of the thickening flow dependence. Water Res. 41 (15), 3359–3371.
Ramin, E., Wágner, D.S., Yde, L., Binning, P.J., Rasmussen, M.R., Mikkelsen, P.S., Plósz, B.G., 2014. A new settling velocity model to describe secondary sedimentation. Water Res. 66, 447–458.
Richardson, J.t., 1954. Sedimentation and fluidisation: Part I. Trans. Inst. Chem. Eng. 32, 35–53.
Samstag, R.W., Ducoste, J.J., Griborio, A., Nopens, I., Batstone, D., Wicks, J., Saunders, S., Wicklein, E., Kenny, G., Laurent, J., 2016. CFD for wastewater treatment: an overview. Water Sci. Technol. 74 (3), 549–563.
Smagorinsky, J., 1963. General circulation experiments with the primitive equations: I. The basic experiment. Mon. Weather Rev. 91 (3), 99–164.
Stickland, A.D., 2015. Compressional rheology: a tool for understanding compressibility effects in sludge dewatering. Water Res. 82, 37–46.
Takacs, I., Patry, G.G., Nolasco, D., 1991. A dynamic model of the clarification-thickening process. Water Res. 25 (10), 1263–1271.
Tchobanoglous, G., Stensel, H.D., Tsuchihashi, R., Burton, F.L.F.L., Abu-Orf, M., Bowden, G., Pfrang, W., 2014. Wastewater Engineering Treatment and Resource Recovery/Metcalf and Eddy, AECOM, fifth edition/revised by George Tchobanoglous, H. David Stensel, Ryujiro Tsuchihashi, Franklin Burton; contributing authors, Mohammad Abu-Orf, Gregory Bowden, William Pfrang. McGraw-Hill Higher Education, New York, NY.
Tee, S.-Y., Mucha, P., Cipelletti, L., Manley, S., Brenner, M., Segre, P., Weitz, D., 2002. Nonuniversal velocity fluctuations of sedimenting particles. Phys. Rev. Lett. 89 (5), 054501.
Torfs, E., Martí, M.C., Locatelli, F., Balemans, S., Bürger, R., Diehl, S., Laurent, J., Vanrolleghem, P.A., François, P., Nopens, I., 2017. Concentration-driven models revisited: towards a unified framework to model settling tanks in water resource recovery facilities. Water Sci. Technol. 75 (3), 539–551.
Valle Medina, M., Laurent, J., 2020. Incorporation of a compression term in a CFD model based on the mixture approach to simulate activated sludge sedimentation. Appl. Math. Model. 77, 848–860.
Vesilind, P.A., 1968. Design of prototype thickeners from batch settling tests. Water Sewage Works 115 (7), 302–307.